19th Brazilian Congress of Thermal Sciences and Engineering
November 6th–10th, 2022, Bento Gonçalves - RS - Brazil

ENC-2022-0594
STUDY OF COMPRESSIBLE DIRECT NUMERICAL SIMULATIONS OF WAVE PACKETS INTERACTING WITH BUMPS

Ana Elisa Basilio de Carvalho[1]
Fernando H T Himeno[2]
Marlon Sproesser Mathias[3]
Marcello Augusto Faraco de Medeiros[4]
[1 2 4] São Carlos School of Engineering, University of São Paulo, EESC-USP.
[3] Institute of Advanced Studies, USP.
[1] anaelisabasilio@usp.br, [2] fernando.himeno@usp.br, [3] marlon.mathias@usp.br, [4] marcello@sc.usp.br

Abstract. *Through Direct Numerical Simulations (DNS), this work investigates the boundary layer stability of two-dimensional wave packets over a smooth plate with a two-dimensional isolated bump immersed in a compressible laminar boundary layer flow. The objective of the current work is to develop a suitable two-dimensional mesh with the DNS code for hydrodynamic instability analysis on different Mach numbers. The numerical simulations were performed by a high order DNS for the compressible Navier-Stokes equations, developed by the Group of Aeroacoustics, Transition and Turbulence (GATT) of the Department of Aeronautical Engineering of the São Carlos School of Engineering, University of São Paulo (EESC-USP). A rectangular bump is positioned on a smooth plate. Five different bumps were defined by their height, proportional to the boundary layer displacement thickness at the position of the center of the bump on the smooth plate, that is, 0.05, 0.1, 0.2, 0.3 and 0.4. Upstream from the bump, there is a region capable of generating disturbances that travel downstream, interacting with the bump. For each height, a different base flow was generated, as well as for each Mach number on the subsonic and transonic regimes, 0.1, 0.3, 0.6, 0.7, 0.8 and 0.9. For each base flow, a wave packet type of disturbance was introduced into the boundary layer through an acoustic source, which is composed by a band of Fourier modes, presenting a narrow range of frequencies exited at different amplification rates.*

Keywords: *bump, wave packet, Direct Numerical Simulation, boundary layer stability*

1. INTRODUCTION

In the aeronautical industry, structures similar to small bumps on a smooth surface, or an isolated roughness on a flat plate, are commonly present on aircraft surfaces, and can influence the drag coefficient if there is transition to the turbulent regime in the boundary layer. Even with a relatively small influence, preventing multiple sources like these is an interesting study that can be beneficial in saving fuel and operating costs.

The boundary layer transition is a process that can be initiated by instabilities. There is a large number of factors that influence on transition, several of which are interdependent. The study of each aspect individually promotes a better understanding of the complete mechanism and allows predictive modeling of phenomena, a great advantage in the aeronautical industry. In boundary layer flows, transition is often caused by primary instabilities and, as a consequence, the amplification of secondary instabilities.

Through Direct Numerical Simulations (DNS), the objective of the current work is to develop a suitable two-dimensional mesh and investigate the effects of two-dimensional wave packets over a flat plate with a two-dimensional isolated roughness element immersed in a compressible laminar boundary layer flow.

2. REVIEW

Early works investigated roughness elements and isolated imperfections on the surface of airfoils with zero pressure gradient or flat plates as factors that promoted transition from laminar to turbulent flow. Wind tunnel experiments from Fage (1943), Tani (1961, 1969) and those shown in the review by Dryden (1953) indicated that a smoother surface influenced in the conservation of stability in a laminar boundary layer. Therefore, to conserve laminar flow it was of great importance to establish the highest height h of the structures that could be tolerated without influencing the transition. For some combinations of roughness height-thickness ratio dependent, stream speed and location of roughness element,

it was also determined that, for higher flow speeds, the distance between roughness and the transition point was gradually reduced.

On studies about two-dimensional roughnesses with disturbances, such as Klebanoff and Tidstrom (1972), Dovgal and Kozlov (1990), Morkovin (1990) and Wörner *et al.* (2003) , it was concluded that the flow region modified by the presence of the roughness is more sensitive to destabilizing influences. The degree of instability was dependent on the velocity profile and its interaction with the roughness geometry. The presence of waves with small oscillation amplitudes in the roughness region, around 1% of the velocity on the outer edge of the boundary layer U_0, already proved strong influence on transition.

In stability theory for compressible flows, the primary interest is in unstable rather than neutral waves (Mack, 1987). The maximum spatial amplification rate as a function of Mach for 2D waves indicates that the second and higher modes are most unstable as 2D waves, because they depend on the thickness of the relative supersonic region, but the first mode is most unstable as an oblique wave at all supersonic Mach numbers. For lower Mach numbers, an oblique wave can have an amplification rate several times larger than a 2D wave. For $M < 2.4$, an oblique first-mode wave is even more unstable than a 2D second-mode wave. For Dunn and Lin (1955) as the Mach Number increases, three-dimensional disturbances become significant under conditions that are less and less extreme, until finally, at a Mach Number between one and two, they begin to play the leading role in many cases of practical interest.

Results in Lees (1947) and Lees and Reshotko (1962) indicate that, for the laminar boundary layer flow, the minimum critical Reynolds number decreases from its Mach number zero value, reaches a minimum somewhere around $M = 3$ and then increases again. In Criminale *et al.* (2018), it is shown that up to $M = 1.6$, the neutral stability curve is quite similar to the incompressible case, but at higher values of the Mach number the upper branch turns upward toward the inviscid limit. As pointed out by Mack in his calculations, inviscid disturbances begin to dominate at $M = 3$ and the stability characteristics are more like those of a free shear layer than of a low-speed zero-pressure gradient boundary layer.

3. METHODOLOGY

The numerical simulations were performed by a DNS for the compressible Navier-Stokes equations, developed by the Group of Aeroacoustics, Transition and Turbulence (GATT) of the Department of Aeronautical Engineering of the São Carlos School of Engineering, University of São Paulo (EESC-USP). The main works that present the development and validation of the DNS can be found in Bergamo (2014), Gaviria Martínez (2016), Mathias (2017), Mathias and Medeiros (2019).

In this work, the fourth order Runge-Kutta method is used for time marching. For the spatial derivatives, a sixth order compact spectral-like compact finite differences shown by Lele (1992) is used. The pre processing is done in MATLAB and the main processing is written in FORTRAN.

The governing equations were defined in a two-dimensional domain (x, y), and time (t), in terms of density (ρ), the two velocity components (u, v), and internal energy (e). The values presented here are non-dimensional, by the characteristic velocity at the outer edge of the boundary layer (U_0), the boundary layer displacement thickness at the roughness position (δ^*_R) and initial density (ρ_0).

For the boundary conditions, the inflow boundary is defined as an uniform flow at constant temperature and the pressure derivative is zero. In the outflow, pressure is kept constant and the second derivative is null for the other variables. The outer flow condition on the wall-normal direction sets the second derivative of all variables to zero.

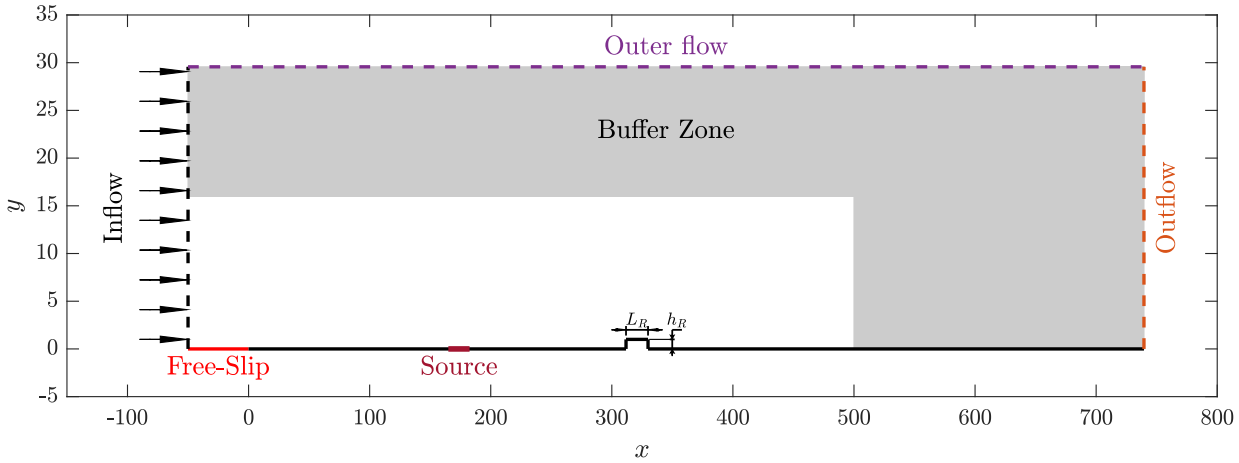

Figure 1. Illustration of the domain (non-dimensional)

For the walls, including the roughness, there are no-slip and no-penetration conditions for velocity, the pressure gradient is zero in the normal direction and the temperature is fixed. From $x = -50$ to $x = 0$ there is a free-slip region in the wall, necessary to accommodate the flow before the boundary layer starts forming.

A rectangular roughness placed on a flat plate, according to Fig. 1. Upstream from the roughness, there is a region capable of generating disturbances that travel downstream, interacting with the roughness.

Some flow parameters were taken from the experimental works by de Paula (2007) and de Paula *et al.* (2017), such as: Reynolds number in the position of the wave source $Re_{\delta^*_{TS}} = 700$, Reynolds number at the roughness position $Re_{\delta^*_R} = 950$, roughness diameter $d = 10\ mm$ and displacement thickness at the experimental roughness location $\delta^*_R = 0.55\ mm$.

Five different bumps were defined by their height, proportional to the boundary layer displacement thickness at the position of the center of the bump on the smooth plate, that is, $\delta^*_R = 0.05, 0.1, 0.2, 0.3$ and 0.4. The initial condition is a Blasius boundary layer at constant temperature and pressure. The characteristic Reynolds number is $Re = 950$.

The meshes are Cartesian and initially uniform, which can be stretched in certain regions, increasing the density of nodes as needed, as seen on Fig. 2 and 3. For the flows with the roughness element, the mesh is refined in the x direction around the roughness region. In the y direction it is refined on the boundary layer region, and extra refined around the height of the roughness.

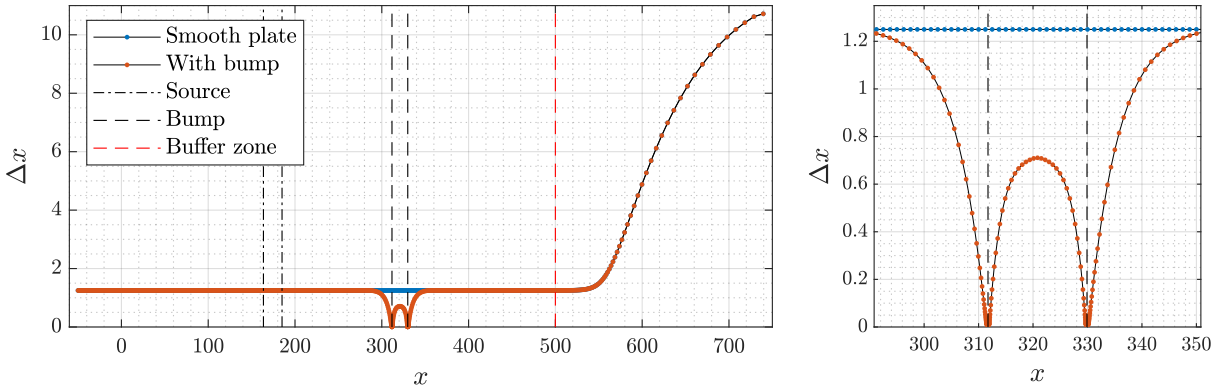

Figure 2. Mesh spacing (stream-wise direction)

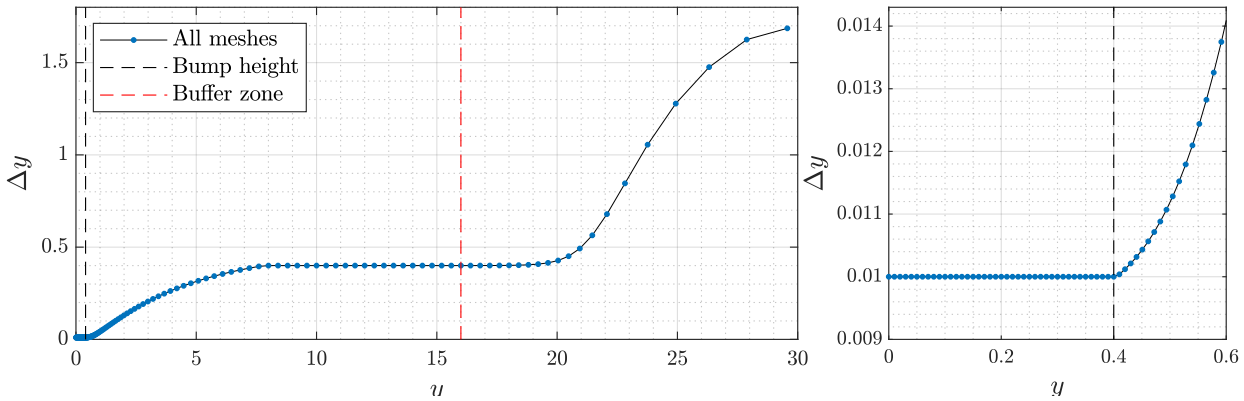

Figure 3. Mesh spacing (wall-normal direction)

The buffer zone consists of the region from $x = 500$ to the end of the mesh, which is included to avoid problems in the simulation, such as reflections in the domain. In y, there is a region with an intense refinement along the height of the roughness, from $y = 0$ to $y = 0.4$. The buffer zone starts at $y = 16$ and ends at the last node.

4. RESULTS

The results will be presented for $M = 0.1, 0.3, 0.6, 0.7, 0.8$ and 0.9. For each Mach number, a different base flow was generated for the flat plate and for the each plate with an isolated roughness, for comparison. Then, for all the base flows, it was introduced a wave packet type of disturbance into the boundary layer through an acoustic source, which is composed by a band of Fourier modes, presenting a narrow range of frequencies exited at different amplification rates.

4.1 Base Flow

The simulation of flat plate with roughness has a maximum relative error close to the order of 10^{-12}, an adequate value for a base flow simulation for the following analysis. In Fig. 4 and 5, the displacement and momentum thickness of the boundary layer, respectively, were calculated using the equations in Schlichting and Gersten (2017).

The roughness effects are proven to mostly local, but seem to expand downstream from the element as the Mach number grows. For higher M, these values do not return to the flat plate values within the physical domain. It seems that the roughness height effects remain similar as the M changes. The distortion is also greater in value for θ as the Mach number grows, the opposite of what is shown for δ^*. The curve format changes noticeably specially for θ from the increasing M, and as from $M = 0.8$, the height also contributes to this.

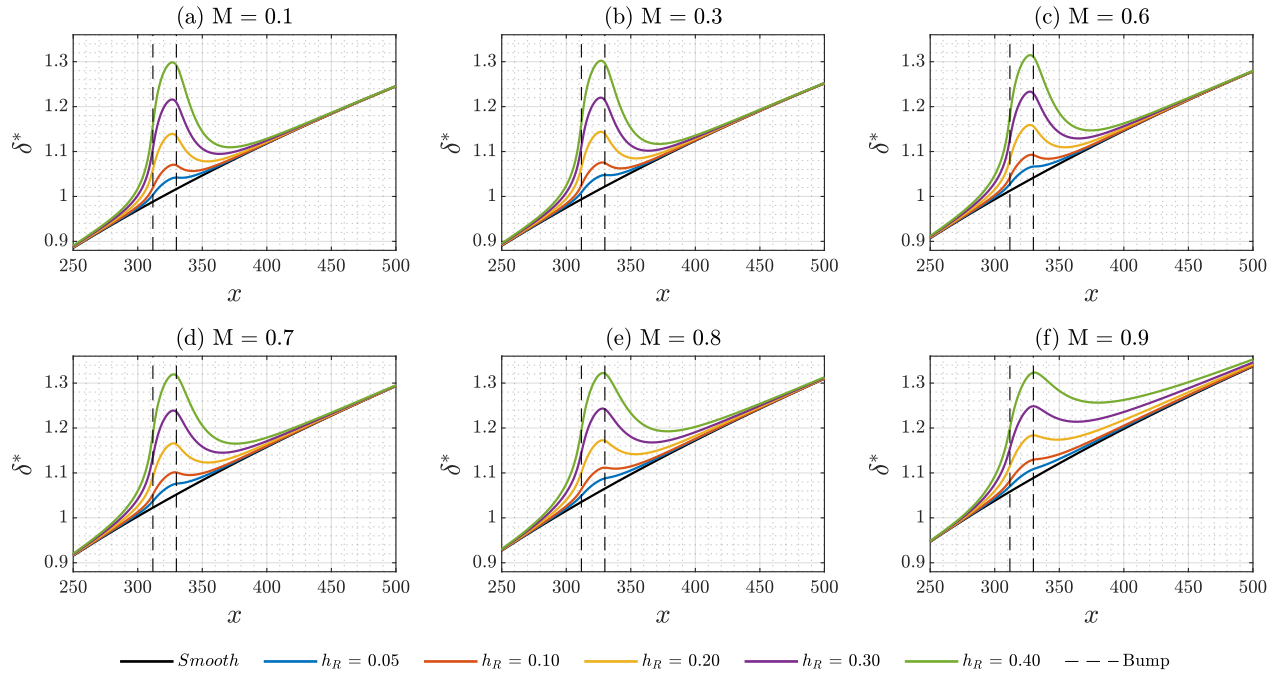

Figure 4. Displacement thickness on the boundary layer for the base flows

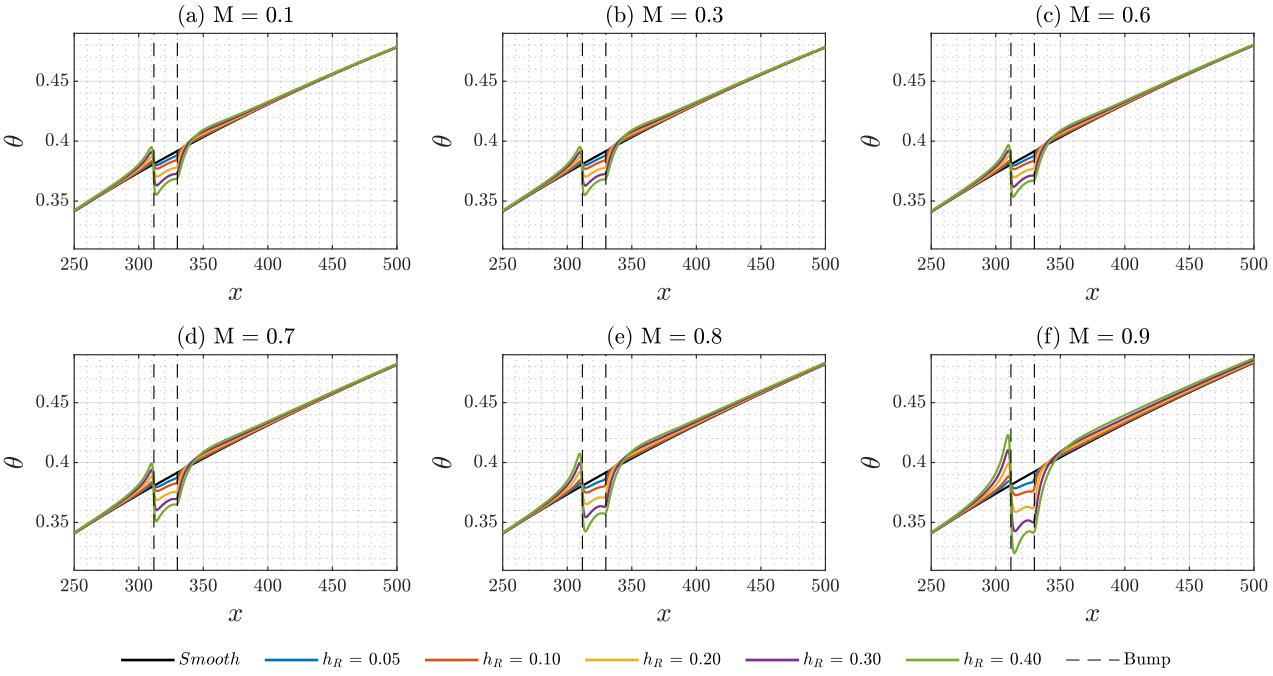

Figure 5. Momentum thickness on the boundary layer for the base flows

4.2 Disturbed Flow

A Gaussian shaped function is used to introduce the wave packet excitation disturbance along the x direction. Along time, a sum of periodic functions compose the signal. The frequency bandwidth of this signal controls the simulation time needed to introduce the complete disturbance. The lower the fundamental mode, the higher the simulation time required to introduce the full signal. In order to shorten this time, after the summation a Gaussian function is applied establishing a smooth threshold. In this work, there are 40 modes at regular frequency intervals, starting at $F_0 = 5 \times 10^{-6}$. The physical and spectral space of such function are shown in Fig. 6.

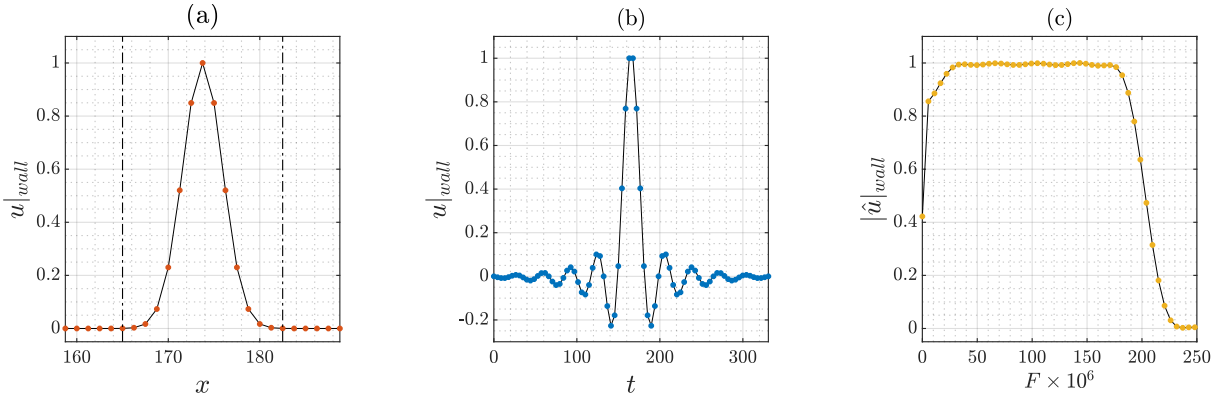

Figure 6. Wave packet signal at wall

It is also necessary to ensure that the distance between excitation and bump is sufficient to the wave packet development. Fig. 7 shows the wave packet evolution for $M = 0.1$ along a smooth plate and $h_R = 0.40$, for comparison. The chosen stations correspond to intermediate positions between an excitation source and the end of the regular mesh, with one station corresponding exactly to the bump center location, x_R. The amplitude increases as the bump height does, as already shown by Wörner *et al.* (2003).

It is seen that the results for the plate with a bump are stretched out in the frequency domain, covering slightly higher values, as well as much more amplified in relation to the smooth plate.

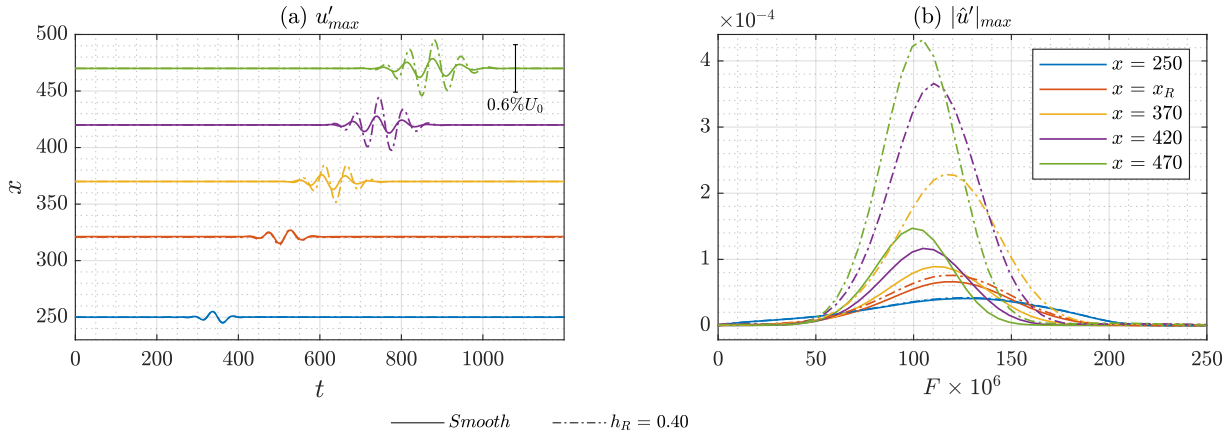

Figure 7. Amplitude evolution $|\hat{u}'|_{max}$ and FFT between the smooth plate and $h_R = 0.40$, for $M = 0.1$

The same analysis is now extended by comparing the results of low Mach regime, $M = 0.1$, to that obtained for 0.3, 0.6, 0.7, 0.8 and 0.9. The effect of bump height change at these Mach numbers are shown in Fig. 8 comparing the smooth case to the bumps. It seems that the tendency from $M = 0.1$ of a longer signal as the height increases is maintained for higher Mach numbers.

For heights up to $h_R = 0.10$, the change in amplitude values is quite small, being very similar to the smooth plate. In this scenario, as Mach increases the selected mode becomes more stable. For the higher bumps, up from $h_R = 0.20$, the difference is more noticeable. For higher heights the amplitude change is quite different from the smooth one. The height itself is responsible for considerable part of this change. It can be noted that for higher bumps the amplitude evolution also changes compared to that from smooth.

The evolution of the wave format downstream is relatively kept for every height within each Mach number. This requires another type of visualization for these results as to distinguish their effects.

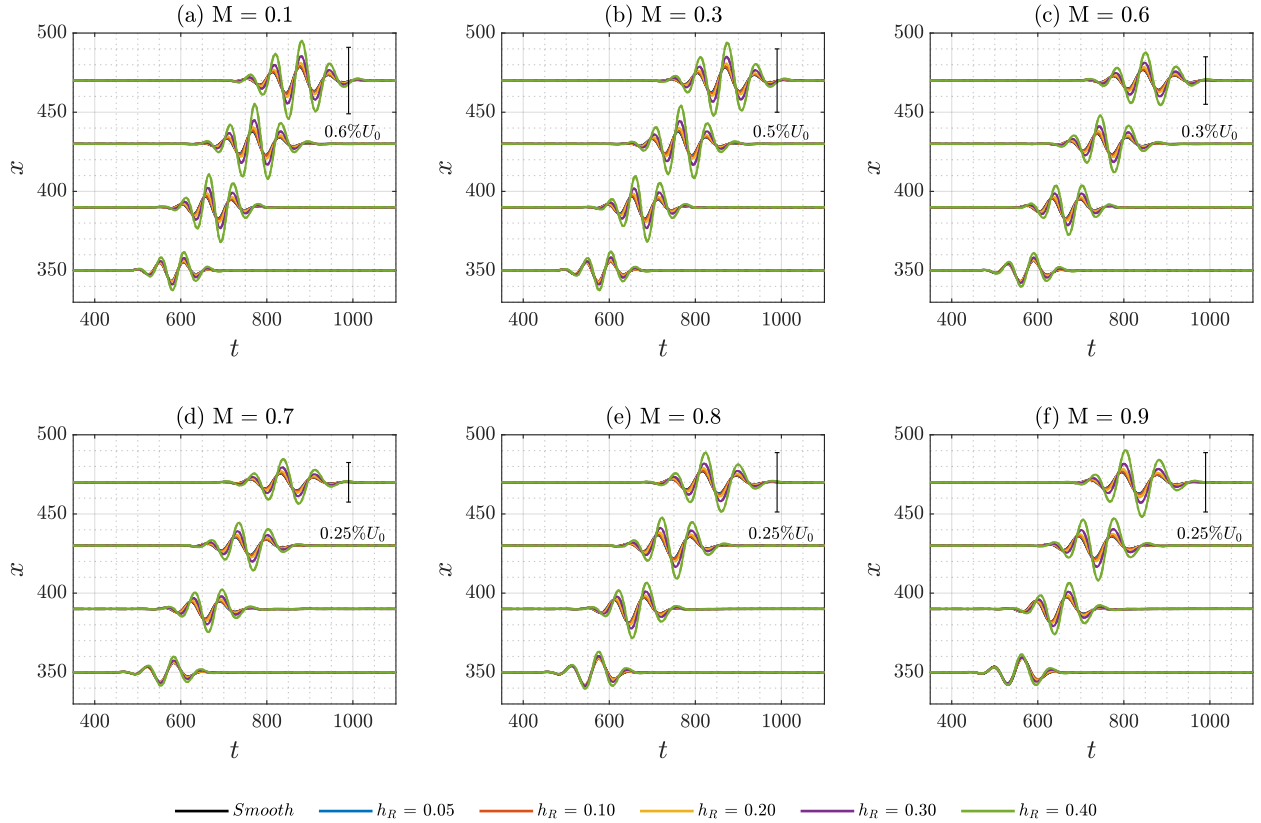

Figure 8. Amplitude evolution $|\hat{u}'|_{max}$

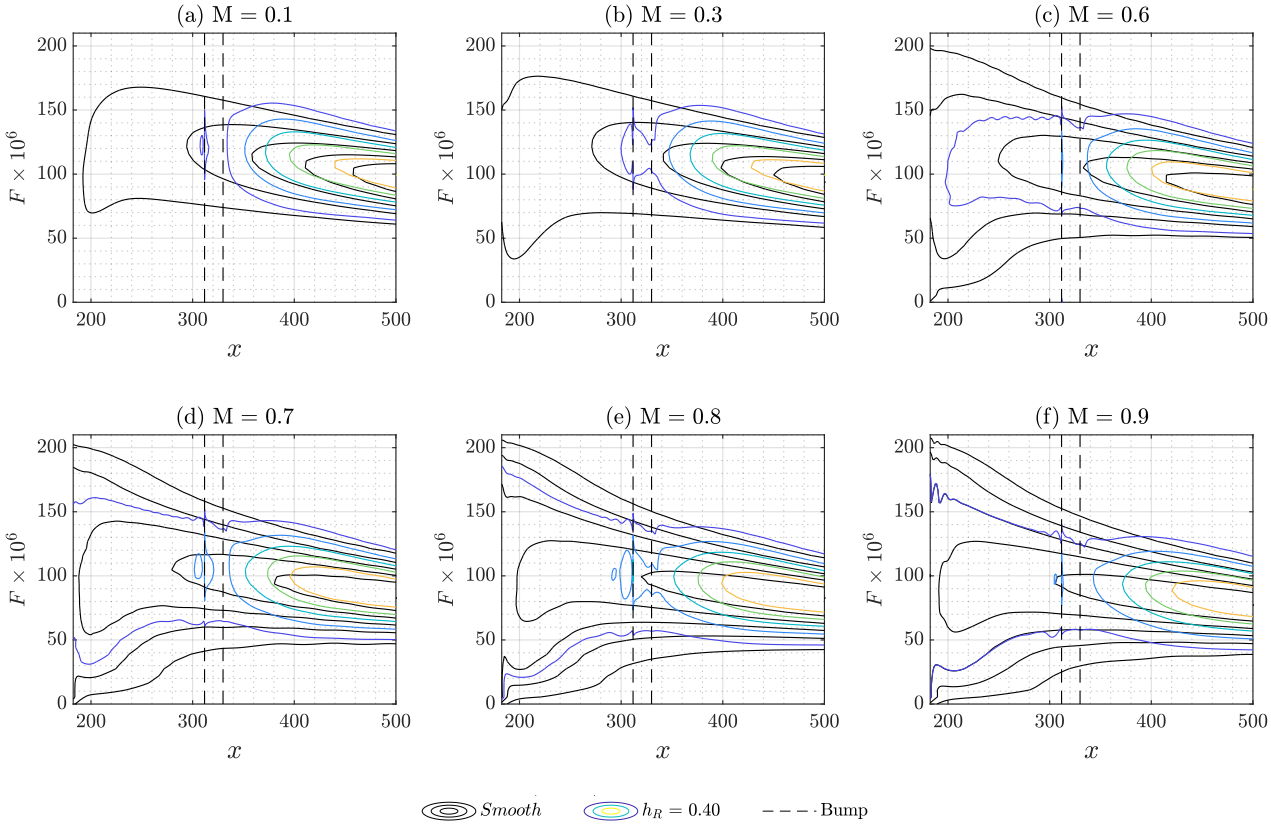

Figure 9. Amplitude $|\hat{u}'|_{max}$ between the smooth plate and $h_R = 0.40$

Figure 9 shows the amplitude in regular intervals between its minimum and maximum values for each Mach number. The black lines represent the smooth plate and the colorful lines are the tallest bump, with $h_R = 0.40$. The bump location is also indicated by the dashed lines. With this, it is now clear that there is indeed a slight shift in the frequency domain as the bump height increases, towards higher F.

The higher the Mach number, the lower is the frequency of maximum amplification, so the unstable band shifts to lower frequencies. Thus, the amplification of the unstable band becomes wider with bumps of heights over and equal to $h_R = 0.10$.

It is also noted that, between the same bump heights, the maximum amplitude value decreases as the Mach number increases. Additionally, comparing the maximum amplitude between heights for the same Mach number, the amplitude steadily increases with h_R.

5. CONCLUSIONS

Through Direct Numerical Simulations (DNS), this work investigates the boundary layer stability of two-dimensional wave packets over a flat plate and plates with a two-dimensional isolated roughness element, immersed in a compressible laminar boundary layer flow.

The influence of Mach number on the effect of a bump on the TS wave evolution has not been yet addressed systematically. Here, it was found that for bump heights below 10%, the effect was comparatively independent on frequency. Above it, the effect of the bump increased with the frequency. The frequency influence is larger at higher Mach numbers and higher bump heights.

However, the effect at the roughness location is relatively small. The Mach effect is mostly a consequence of the downstream region affected by the bump, which increases substantially, in particular when approaching the transonic regime.

6. ACKNOWLEDGEMENTS

This study was financed in part by the Coordenação de Aperfeiçoamento de Pessoal de Nível Superior - Brasil (CAPES) - Finance Code 001 and by São Paulo Research Foundation (FAPESP/Brazil) - project grant 2019/15336-7.

Research carried out using the computational resources of the Center for Mathematical Sciences Applied to Industry (CeMEAI) funded by FAPESP (grant 2013/07375-0).

F.H.T.H is sponsored by São Paulo Research Foundation (FAPESP/Brazil) grant #2018/02542-9.

M.S.M. is sponsored by São Paulo Research Foundation (FAPESP/Brazil) grant #2018/04584-0.

M.A.F.M. is sponsored by National Council for Scientific and Technological Development (CNPq/Brazil), grant #307956/2019-9.

We would like to thank the US Air Force Office of Scientific Research (AFOSR), grant FA9550-18-1-0112, managed by Dr. Geoff Andersen from SOARD (Southern Office of Aerospace Research and Development).

7. REFERENCES

Bergamo, L.F., 2014. *Instabilidade hidrodinâmica linear do escoamento compressível em uma cavidade*. Master's thesis.

Criminale, W.O., Jackson, T.L. and Joslin, R.D., 2018. *Theory and Computation in Hydrodynamic Stability*. Cambridge University Press.

de Paula, I.B., Würz, W., Mendonça, M.T. and Medeiros, M.A.F., 2017. "*Interaction of instability waves and a three-dimensional roughness element in a boundary layer*". Journal of Fluid Mechanics, Vol. 824, pp. 624–660.

de Paula, I.B., 2007. *Influência de uma rugosidade tridimensional isolada na transição de uma camada limite sem gradiente de pressão*. Ph.D. thesis, Universidade de São Paulo.

Dovgal, A.V. and Kozlov, V.V., 1990. "*Hydrodynamic Instability and Receptivity of Small Scale Separation Regions*". Laminar-Turbulent Transition, pp. 523–531.

Dryden, H.L., 1953. "*Review of Published Data on the Effect of Roughness on Transition from Laminar to Turbulent Flow*". Journal of the Aeronautical Sciences, pp. 447–482.

Dunn, D.W. and Lin, C.C., 1955. "*On the stability of the laminar boundary layer in a compressible fluid*". Journal of the Aeronautical Sciences, Vol. 22, pp. 455–477.

Fage, A., 1943. "*The smallest size of spanwise surface corrugation which affects boundary-layer transition on an airfoil*". Aeronautical Research Council, R & M 2120.

Gaviria Martínez, G.A., 2016. *Towards natural transition in compressible boundary layers*. Ph.D. thesis, Universidade de São Paulo.

Klebanoff, P.S. and Tidstrom, K.D., 1972. "*Mechanism by Which a Two-Dimensional Roughness Element Induces Boundary-Layer Transition*". The Physics of Fluids, Vol. 15, No. 7, pp. 1173–1188.

Lees, L., 1947. "*The stability of the laminar boundary layer in a compressible fluid*". NACA TR-876.

Lees, L. and Reshotko, E., 1962. "*Stability of the compressible laminar boundary layer*". Journal of Fluid Mechanics, Vol. 12, p. 555–590.

Lele, S.K., 1992. "*Compact Finite Difference Schemes with Spectral-like Resolution*". Journal of Computational Physics, Vol. 106, pp. 16–42.

Mack, L., 1987. "*Review of compressible stability theory*". In *Stability of time dependent and spatially varying flows*. Springer.

Mathias, M.S., 2017. *Instability analysis of compressible flows over open cavities by a Jacobian-free numerical method*. Master's thesis, Universidade de São Paulo.

Mathias, M.S. and Medeiros, M.F., 2019. *Global instability analysis of a boundary layer flow over a small cavity*.

Morkovin, M.V., 1990. "*On Roughness-Induced Transition: Facts, Views, and Speculations*". pp. 281–295.

Schlichting, H. and Gersten, K., 2017. *Boundary-Layer Theory*. Springer, Berlin, Heidelberg.

Tani, I., 1961. "*Effect of Two-Dimensional and Isolated Roughness on Laminar Flow*". Boundary Layer and Flow Control, Vol. 2, pp. 637–656.

Tani, I., 1969. "*Boundary Layer Transition*". Annual Review of Fluid Mechanics, Vol. 1, pp. 169–196.

Wörner, A., Rist, U. and Wagner, S., 2003. "*Humps/Steps Influence on Stability Characteristics of Two-Dimensional Laminar Boundary Layer*". AIAA Journal, Vol. 41, No. 2, pp. 192–197.

8. RESPONSIBILITY NOTICE

The authors are solely responsible for the printed material included in this paper.